Biochimica et Biophysica Acta 1853 (2015) 733–745

Contents lists available at ScienceDirect

Biochimica et Biophysica Acta

journal homepage: www.elsevier.com/locate/bbamcr

Reticulon protein-1C is a key component of MAMs

Valentina Reali [a,1], Bisan Mehdawy [b,1], Roberta Nardacci [c], Giuseppe Filomeni [d], Anna Risuglia [a], Federica Rossin [a], Manuela Antonioli [a,c], Claudia Marsella [a,c], Gian Maria Fimia [c,e], Mauro Piacentini [a,c,*], Federica Di Sano [a,**]

[a] Department of Biology, University of Rome 'Tor Vergata', Via della Ricerca Scientifica, 00133 Rome, Italy
[b] European Centre for Brain Research, IRCSS Santa Lucia Foundation, Via del Fosso di Fiorano 64, 00143 Rome, Italy
[c] National Institute for Infectious Diseases, IRCCS 'L. Spallanzani', Via Portuense, 00149 Rome, Italy
[d] Cell Stress and Survival Unit, Danish Cancer Society Research Center, Strandboulevarden 49, 2100 Copenhagen, Denmark
[e] Department of Biological and Environmental Sciences and Technologies (DiSTeBA), University of Salento, Lecce, Italy

ARTICLE INFO

Article history:
Received 19 October 2014
Received in revised form 17 December 2014
Accepted 27 December 2014
Available online 5 January 2015

Keywords:
RTN-1C
Endoplasmic reticulum
MAM
Mitochondria

ABSTRACT

The endoplasmic reticulum (ER) is a key organelle fundamental for the maintenance of cellular homeostasis and the determination of cell fate under stress conditions. Reticulon-1C (RTN-1C) is a member of the reticulon family proteins localized primarily on the ER membrane and known to regulate ER structure and function. Several cellular processes depend on the structural and functional crosstalk between different organelles, particularly on the endoplasmic reticulum and mitochondria. These dynamic contacts, called mitochondria-associated ER membranes (MAMs), are essential for the maintenance of mitochondrial structure and participate in lipid and calcium exchanges between the two organelles.
In this study we investigated the impact of RTN-1C modulation on mitochondrial dynamics. We demonstrate that RTN-1C controls mitochondrial structure and function affecting intracellular Ca^{2+} homeostasis and lipid exchange between ER and mitochondria. We propose that these events depend on RTN-1C involvement in the regulation of ER–mitochondria cross-talk and define a role for RTN-1C in maintaining the function of contacts between the two organelles.

1. Introduction

The presence of contact points between ER and mitochondria has been known for many years [1] and has been studied in different systems with different techniques [2–4].

This special compartment, defined as "mitochondria-associated ER membrane" (MAM), is involved in several important metabolic cellular functions [5] including phospholipid metabolism and calcium homeostasis [6,7] as well as the pathogenesis of various human diseases [8,9].

One of the major functions of MAM is the control of Ca^{2+} signaling between the ER and mitochondria. In fact, although ER is considered the main calcium store in the cell, mitochondria also play an important role in Ca^{2+} homeostasis particularly in neuronal cells where it has been demonstrated that calcium-dependent pathways are closely related to the onset of chronic and acute diseases. Interestingly recent reports have shown the importance of mitochondrial Ca^{2+} up-take via MAM. In fact it has been demonstrated that the mitochondrial network regulates Ca^{2+} homeostasis as well as mitochondrial Ca^{2+} up-take depending on their contact sites with ER.

Temporally and spatially organized calcium waves in the cytosol, mitochondria, and nucleus are among the most commonly recognized intracellular signals. However, prolonged disturbances in calcium homeostasis can initiate signaling cascades that eventually lead to cell death [10]. Endoplasmic reticulum (ER) is the main site of intracellular calcium storage. Given ER's prominent role in protein folding and its influence on Ca^{2+}-dependent signaling pathways, disruption of ER function, a condition called 'ER stress', has severe consequences for the cell [11].

Mitochondria within living cells are highly dynamic. Indeed, it is clear that mitochondria can undergo fission and fusion [12]. The disruption of this dynamic equilibrium may contribute to cell injury or death underlying developmental and neurodegenerative disorders. Mitochondrial fusion was suggested as a complementation mechanism which allows mitochondria to compensate for reduced mitochondrial bioenergetic efficiency under conditions of energy deprivation [13]. In this regard, it was recently demonstrated that mitochondria unexpectedly elongate during the activation of autophagy [14].

Reticulons (RTNs) are a family of proteins mainly localized on the endoplasmic reticulum [15]. Previous work suggested that cells overexpressing the reticulon protein-1C (RTN-1C), are more sensitized to

* Correspondence to: M. Piacentini, Department of Biology, University of Rome 'Tor Vergata', Via della Ricerca Scientifica, 00133 Rome, Italy.
** Corresponding author. Tel.: +39 0672594232; fax: +39 062023500.
E-mail address: federica.di.sano@uniroma2.it (F. Di Sano).
[1] Co-first authors.

http://dx.doi.org/10.1016/j.bbamcr.2014.12.031
0167-4889/

apoptosis, possibly as a consequence of ER stress [16]. Neuroblastoma cells overexpressing RTN-1C showed an enlargement of the ER membranes which was paralleled by enhanced levels of cytosolic Ca^{2+} due to its leak from the ER lumen to the cytosol thus supporting the notion that RTN-1C induces ER stress. Interestingly, the same cell line displayed mitochondrial ultrastructural alterations mainly characterized by disruption of the matrix and the presence of spared cristae [17].

Based on these findings, here we have studied the role of RTN-1C on mitochondrial morphology and function. It is worth noting that, we provide evidence supporting the notion that the RTN-1C-induced morphological and functional changes of the mitochondria are very likely dependent on the modulation of ER–mitochondria cross-talk.

2. Materials and methods

2.1. Cell lines, transfections and treatments

SH-SY5Y human neuroblastoma and SK-MEL110 melanoma cell lines were grown in Ham's F12 (Lonza,Verviers Belgium) or Dulbecco's modified Eagle's medium (Lonza,Verviers Belgium) respectively, supplemented with 10% fetal bovine serum (Life Technologies, Paisley, UK) in a humidified atmosphere of 5% CO_2 in air.

SH-SY5Y neuroblastoma cells carrying a tetracycline-regulated RTN-1C expression system (SH-SY5Y^{RTN-1C}) were previously obtained in our laboratory [17], and were maintained in the same growth conditions as SH-SY5Y except for the presence of 10% tetracycline-free FBS.

For transient transfections, cells were approximately seeded at 80% confluence and transfected 24 h later with each expression vector by using Xfect™ transfection reagent (Clontech Laboratories, Mountain View, CA, USA) according to the manufacturer's instructions.

The Flag-HA-tagged RTN-1C was obtained from a cDNA human brain library by PCR amplification using specific primers and fragments were cloned into pcDNA4/TO vector (Invitrogen, Life Technologies Ltd, Paisley, UK). SK-MEL110 were stably transfected with Lipofectamine 2000 (Invitrogen) with pcDNA4/TO RTN-1C construct together with the pcDNA6/TR vector. Stable transformants were established by selection with zeocin (1 ng/ml) and blasticidin (10 μg/ml) (Invitrogen).

For Ca^{2+} measurement experiments, SH-SY5Y cells were grown on glass coverslips and transfected with 0.5 μg mitochondrially targeted ratiometric pericam (2mtRP) targeted to the inner mitochondrial membrane using the targeting sequence of subunit VIII of cytochrome C oxidase (Gift from Dr. Tullio Pozzan). A total of 1 μg DNA and 1.5 μl Lipofectamine2000 (Invitrogen) was added to cells for 24 h, before medium was replaced. Where RTN-1C was construct was used in conjunction with 2mtRP a DNA ration of 1:1 was used.

2.2. Tandem affinity purification

2.0×10^7 of cells were lysed in TAP buffer (10 mM Tris pH 8.0, 150 mM NaCl, 10% Glycerol, 0.5% NP-40). Equal amounts of protein extracts were immunoprecipitated using anti-Flag agarose beads (Sigma-Aldrich). Immunocomplexes were eluted with a Flag peptide (Sigma-Aldrich) at 0.2 mg/ml of concentration. A second immunoprecipitation was performed on the eluted proteins using anti-HA agarose beads (Sigma-Aldrich) and proteins were finally eluted by incubation with glycine 100 mM pH 2.4. Proteins were digested with trypsin as described [18]. Resulting peptide mixtures were analyzed by LC/MALDI-TOF-TOF mass spectrometry as described [19].

2.3. RNA-interference 'knockdown' of RTN-1C

For RNA-interference 'knockdown' of RTN-1C, SH-SY5Y cells were transiently transfected for 48 h with The Ambion Custom Select siRNA (small interfering RNA) specific for RTN-1C (siRNA-RTN-1C) and a scrambled sequence (scRNA) (Ambion, Life Technologies Ltd, Paisley, UK). Each siRNA was trasfected with Xfect™ transfection reagent (Clontech Laboratories, Mountain View, CA, USA) according to the manufacturer's instructions.

2.4. Microscopy

2.4.1. Immunofluorescence

Cells were grown on poly-L-lysine-coated sterile glass slide. RTN-1C was induced for 24 h and 48 h with Doxy at 1 μg/ml concentration. After medium removal, cells were washed twice in PBS, thereafter fixed in 4% parafolmaldehyde-PBS for 10 min, and then permeabilized for 10 min with 0.1% Triton X-100. Next, cells were rinsed three times with PBS and nonspecific binding sites were blocked in PBS/10% FBS for 30 min. Appropriate primary antibodies were added for 1 h dissolved in PBS/1% FBS solution. We used anti-RTN-1C mouse (1:500; Abcam, Cambridge, UK), anti-ATP synthase rabbit (1:250; Sigma, St Louis, MO, USA), and anti-Facl4 goat (1:50; Santa Cruz Biotechnology, Dallas, Texas, USA) antibodies. After three washes in PBS, cells were incubated for 30 min with the appropriate anti-mouse, anti-rabbit and anti-goat secondary antibodies (Alexa, Molecular Probes, Monza, Italy) diluted 1:1000 in PBS/1% FBS. Finally, cell nuclei were stained with Hoechst 33342 (Molecular Probes, Monza, Italy). Slides were observed and photographed in a Leica TCS SP2 or Olympus IX81 (with FLUOVIEW 1000 confocal laser system) confocal microscope.

2.4.2. Electron microscopy

Cells were fixed with 2.5% glutaraldehyde (Sigma-Aldrich, R1012) in 0.1 M cacodylate buffer, pH 7.4, for 45 min at 4 °C, rinsed in buffer, postfixed in 1% OsO_4 in 0.1 M cacodylate buffer, pH 7.4, dehydrated, and embedded in Epon resin (Agar Scientific, 45359-1EA-F). Grids were thoroughly rinsed in distilled water, stained with aqueous 2% uranyl acetate for 20 min and photographed in a Zeiss EM 900 electron microscope. The number of mitochondria or the ER–mitochondria contact sides was evaluated. A minimum of 1000 contacts and mitochondria were analyzed by three independent experiments.

2.4.3. Immunogold

Cells were fixed in 2% freshly depolymerised paraformaldehyde and 0.2% glutaraldehyde in 0.1 M cacodilate buffer pH 7.4 for 1 h at 4 °C. Samples were rinsed in the same buffer, partially dehydrated and embedded in London Resin White (LR White, Agar Scientific Ltd.). Ultrathin sections were processed for immunogold technique as previously reported [20] utilizing as primary antibody mouse anti-RTN-1C (1:100 Abcam, Cambridge, UK).

2.4.4. Confocal and Ca^{2+} epifluorescence imaging

Images requiring higher spatial resolution of cells transfected with mito-GFP plasmids were taken on a cooled interline CCD camera (coolsnapEZ—Photometrics) and a confocal CARV LX spinning disk unit using a 63× objective, with an optical depth of 1 μm. Samples were then excited at 488 nm, with emissions collected at 505–530 nm, while being maintained at 37 °C in a Krebs/HEPES buffer (KHB in mM: 10 HEPES, 4.2 $NaHCO_3$, 1.18 $MgSO_4$, 1.18 KH_2PO_4, 118 NaCl, 4.69 KCl, 1.8 $CaCl_2$, 11.7 glucose, pH 7.4) (Sigma, Italy).

Calibrated intracellular Ca^{2+} responses were made by loading cells with 2 μM of Fura-2-AM (Molecular Probes, USA) for an hour at 37 °C in Krebs/HEPES buffer (KHB) and then imaging emissions above 510 nm after excitation at 340 and 380 nm. For epifluorescent measurements of mitochondrial Ca^{2+} fluxes, 2mtRP transfected SH-SY5Y cells were mounted on an inverted epifluorescence microscope (Nikon Ti), maintained at 37 °C in KHB sequentially, excited at 405 and 485 nm, and emissions collected at 535 ± 20 nm. Data were captured on a cooled interline CCD camera (coolsnapEZ—Photometrics,Tucson, USA) and converted to 485/405 pseudocolor ratiometric images using Meta Fluor software (Molecular Devices, USA). Measurements of Ca^{2+} responses were made by calculating the mean (peak minus basal) Ca^{2+} response and are expressed in nanomolar concentrations or mt pericam

emission ratio units for intracellular and mitochondrial Ca^{2+} levels respectively.

2.4.5. BODIPY staining and visualization

BODIPY (D3922, Molecular Probes, Carlsbad, Calif, USA) (excitation wavelength 480 nm, emission maximum 515 nm), was diluted in PBS at a concentration of 1 mg/ml.

Cells were grown on sterile glass slide and after medium removal, were washed twice in PBS, thereafter fixed in 4% parafolmaldehyde-PBS for 10 min. Following fixation, samples were washed 3 times in phosphate buffered saline (PBS) and stained with BODIPY for 30 min. Cell nuclei were stained with Hoechst 33342 (Molecular Probes, Monza, Italy). All samples were mounted in Fluoro Gel w/Dabco (Electron Microscopy Sciences, Hatfield, PA, USA) and covered with glass cover slips.

Lipid bodies were quantified by measuring the intensity of fluorescence and number of spots in the isosurface analyzed by IMARIS 7.7 (Bitplane) and normalized to the number of cells in the respective field.

2.5. Protein analysis

2.5.1. Western blot analysis

Cells were harvested and resuspended in a lysis buffer (10 mM Tris–HCl pH 8, 150 mM NaCl, 10% Glicerol, 0.5% NP40) with freshly added protease inhibitors. Then samples were centrifuged at 13,000 rpm for 15 min and protein quantification was carried out according to the Bradford method, using a Bio-rad protein assay solution (Bio-rad, MI, Italy) and BSA as standard. Protein extracts were separated by SDS-PAGE and transferred on nitrocellulose membrane. After blocking in PBS 5% milk for 1 h, membranes were probed with a specific primary antibody: mouse anti-RTN-1C (1:1000; Abcam, Cambridge, UK), rabbit anti-HA (1:2000; Sigma, St Louis, MO, USA), rabbit anti-ATP synthase (1:1000; Sigma, St Louis, MO, USA), mouse anti-FLAG (1:1000; Sigma, St Louis, MO, USA), goat anti-Facl4 (1:100; Santa Cruz Biotechnology, Dallas, Texas, USA), mouse anti-DRP1 (1:1000; BD Transduction Laboratories, USA), rabbit anti-Fis1 (1:500; AdipoGen, Switzerland), rabbit anti-VDAC, mouse anti-calreticulin, rabbit anti-actin and mouse anti-OPA1 (1:1000; BD Transduction Laboratories, USA). Mouse anti-GAPDH (1:1000; Santa Cruz Biotechnology, Dallas, Texas, USA) was used as loading control. The binding of primary antibodies was detected with secondary peroxidase-conjugated antibodies (1:5000; Bio-rad, MI, Italy), and visualized with the enhanced chemoluminescence system (Bio-rad) by using FluorChem SP machine (Alpha Innotech, Rondburg, South Africa).

2.5.2. Immunoprecipitation

Cells were washed twice with PBS and scraped into lysis buffer [150 mM NaCl, 0.5% NP40, 10% Glicerol, 10 mM Tris–HCl (pH 8)] with freshly added protease inhibitors. After an incubation for 30 min on ice, the lysate was centrifuged at 13,000 rpm for 15 min at 4 °C to remove the insoluble cell debris. The anti-RTN-1C antibody was coupled to protein G (Santa Cruz Biotechnology, Dallas, Texas, USA) for 3 h at 4 °C with continuous rocking. For the preclearing, 1 mg of cellular proteins was incubated with protein G for 3 h at 4 °C with continuous rocking. After this, the cellular proteins were incubated with the antibody-linked beads over night at 4 °C with continuous rocking. The day after the complex was centrifuged at 2000 rpm for 5 min at 4 °C and washed in lyses buffer with protease inhibitors for three times. The beads were boiled in sample buffer at 95 °C for 10 min, and samples were resolved by SDS-PAGE and analyzed by Western blotting as described previously.

2.5.3. Subcellular fractionation

Purification of ER, MAM and mitochondria was performed as described [21]. Briefly, three C57BL/6 male mice, aged 4 months (25 g body weight), were scarified using cervical dislocation. Brains were rapidly excised on an ice-cold plate, pooled and homogenized in 25 mM mannitol, 75 mM sucrose, 0.5% BSA, 0.5 mM EGTA and 30 mM Tris–HCl pH 7.4. The homogenate was used to isolate the different fractions that were quantitated for total protein (Bradford system, Biorad) and analyzed by immunoblot using different specific antibodies.

2.6. Mitochondrial assays

2.6.1. MTT reduction

For MTT assay we used the CellTiter 96 Aqueous One Solution Cell Proliferation Assay (Promega, Madison, WI, USA). MTS tetrazolium compound is bioreduced by cells into a colored formazan product that is soluble in tissue culture medium. Conversion is accomplished by NADPH or NADH produced by dehydrogenase enzymes in metabolically active cells. Briefly, cells were seeded on 96-well plate and after 24 h and 48 h of RTN-1C induction, 20 μl of reagent was added directly to wells. After incubation for 4 h at 37 °C, the absorbance at 490 nm was determined using a 96-well plate reader.

2.6.2. Dy_m measurement and oxygen consumption

Dy_m was analyzed cytofluorometrically taking advantage of the Dy_m-sensitive probe MitoTracker Red (Invitrogen—Molecular Probes, San Giuliano Milanese, Italy). Briefly, cells were incubated with 50 nM of MitoTracker Red for 30 min, washed, trypsinized, resuspended in PBS and analyzed in FL-2 by FACScalibur cytofluorometer.

Oxygen consumption was determined at 25 °C using a Clark-type oxygen electrode equipped with thermostatic control and magnetic stirring. Purified mitochondria [22] were resuspended in 1.5 ml of 'experimental' buffer (125 mM KCl, 10 mM Tris–3-(N-morpholino)propane sulfonic acid, pH 7.4, 10 mM ethylene glycol tetraacetic acid–Tris, pH 7.4, 5 mM glutamate, 2.5 mM malate, 1 mM K_2HPO_4). NADH (1 mM) was used as substrate to evaluate oxygen consumption by Complex I (NADH: dehydrogenase). Then rotenone (5 mM) was added to the mitochondrial suspension in order to inhibit Complex I and to allow the measurement of the sole Complex II (succinate dehydrogenase)-driven oxygen consumption by the addition of 1 mM succinate.

2.7. RT-PCR

RNA was extracted by using Trizol reagent (Invitrogen, USA). cDNA synthesis was generated using the reverse transcription kit (Promega, USA) according to the manufacturer's recommendations (3 μg total RNA). Quantitative PCR reactions were performed with the LightCycler (Roche, Switzerland) thermocycler as previously described [23]. Primer sets for all amplicons were designed using the Primer-Express 1.0 software system (see Supplementary Table S1).

2.8. ATP synthase enzyme activity

Cells were cultured in a T-150 flask and homogenized in a buffer (220 mM Mannitol, 68 mM sucrose, 50 mM PipesKOH ph 7.4, 50 mM KCl, 5 mM EGTA, 2 mM $MgCl_2$, 1 mM DTT and protease inhibitors) to obtain the mitochondrial fraction. The F1F0 ATP synthase extraction from mitochondrial fraction was performed according to the manufacturer's instructions (Abcam, Cambridge, UK). Briefly, 10 μg of 10% detergent-extracts of protein per well was incubated in a 96-well plate at room temperature for 3 h to immunoimmobilize F1F0-ATP synthase. The reaction was monitored by Tecan microplate reader at 340 nm.

3. Results

3.1. RTN-1C interacts with mitochondrial compartment

We have previously demonstrated that the reticulon-1C protein regulates endoplasmic reticulum stress and when overexpressed may

trigger apoptotic cell death pathway [17], although the precise mechanism of action remained unclear.

So as to better characterize the role of RTN-1C we decided to use a proteomic approach to identify its protein interactors. We performed a tandem affinity purification assay (TAP) combined with MALDI-TOF-TOF analysis on a human SK-MEL110 melanoma cell line, which has undetectable level of RTN-1C basal expression, carrying an RTN-1C-HA-Flag expression vector. Interestingly, among the different proteins (see supplementary material) we detected alpha and beta chains of mitochondrial ATP synthase.

To confirm the data obtained we used various experimental approaches. First we immunoprecipitated RTN-1C protein in the SK-MEL110 melanoma cell overexpressing the reticulon protein and we analyzed the immunocomplex for the presence of ATP synthase (Fig. 1a). Subsequently we verified the results by immunoprecipitating endogenous ATP synthase (Fig. 1b) or RTN-1C (Fig. 1b) in human

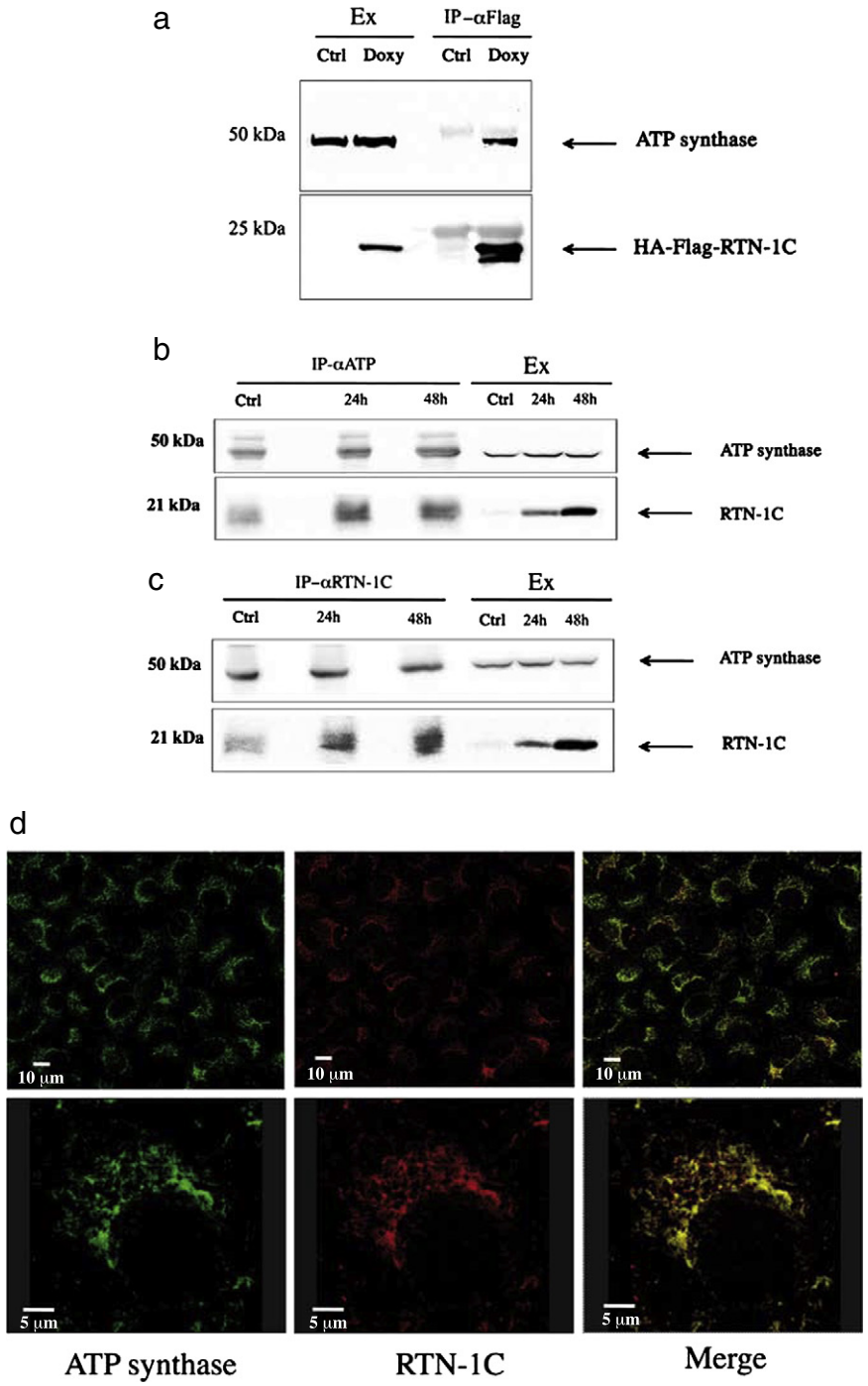

Fig. 1. RTN-1C interacts with mitochondrial ATP synthase. (a) Cell lysates from SK-MEL110 wild-type (ctr) and SK-MEL110-RTN-1C overexpressing cells (48 h doxycycline induction, Doxy) were immunoprecipitated with anti-Flag antibody, subjected to SDS-PAGE and immunoblotting with an anti-ATP synthase antibody (upper panel) and anti-HA antibody (lower panel). Ex: cell extracts. (b, c) Cell lysates from SH-SY5Y wild type and SH-SY5Y^{RTN-1C} cells (24 and 48 h doxycycline induction) were immunoprecipitated with anti-ATP synthase (b) or anti-RTN-1C antibodies (c) and were subjected to SDS-PAGE and immunoblotting with an anti-ATP synthase antibody (upper panels) and anti RTN-1C antibody (lower panels). (d) ATP synthase (green) and RTN-1C (red) staining of SH-SY5Y^{RTN-1C} cells (48 h doxycycline induction) analyzed by confocal microscopy. The yellow staining in the overlaid images indicates the co-localization. Scale bar: upper panels 10 μm, lower panels 5 μm. For Western blot analysis the results shown are representative of three independent experiments.

neuroblastoma SH-SY5Y cells supporting the interaction between the two proteins.

The previous biochemical data were confirmed by immunofluorescence analysis to detect the RTN-1C and ATP synthase cellular localization. Double-immunostaining (Fig. 1d) revealed overlapping areas of RTN-1C and ATP synthase, so indicating a close localization of the two proteins. These results suggested a possible role for the reticulon protein as a contact point for the mitochondrial network.

3.2. RTN-1C modulates mitochondrial activities

We previously showed that mitochondrial compartment of RTN-1C overexpressing cells was as much affected as the endoplasmic reticulum [17]. In particular we demonstrated that RTN-1C overexpression resulted in dilation of the endoplasmic reticulum membranes paralleled by mitochondrial disruption of the matrix and the presence of few spared cristae. In light of the results here obtained we therefore wondered whether RTN-1C was able to regulate mitochondrial activities and homeostasis.

To this end we used an RTN-1C inducible expression system [17] of SH-SY5Y neuroblastoma cell line (SH-SY5Y^{RTN1C}). In these cells we measured mitochondrial transmembrane potential (Dy_m) after doxycycline induction and we found that RTN-1C overexpressing cells have significantly depolarized mitochondria (Fig. 2a and b). Coherently, oxygen consumption measured at the level of Complex I decreased, whereas that measured at the level of Complex II increased (Fig. 2c). These data indicate that mitochondria of RTN-1C overexpressing cells adjust oxidative phosphorylation in order to maintain ATP production (Fig. 2d), by increasing the succinate dehydrogenase activity of Complex II, presumably to counteract an impairment of mitochondrial function.

The RTN-1C effect on mitochondrial activities was also confirmed by measuring the MTT conversion by mitochondrial enzymes in RTN-1C overexpressing cells as an indication of mitochondrial function. We found that the increase in reticulon protein significantly reduced mitochondrial activity in comparison to controls (Fig. 2e).

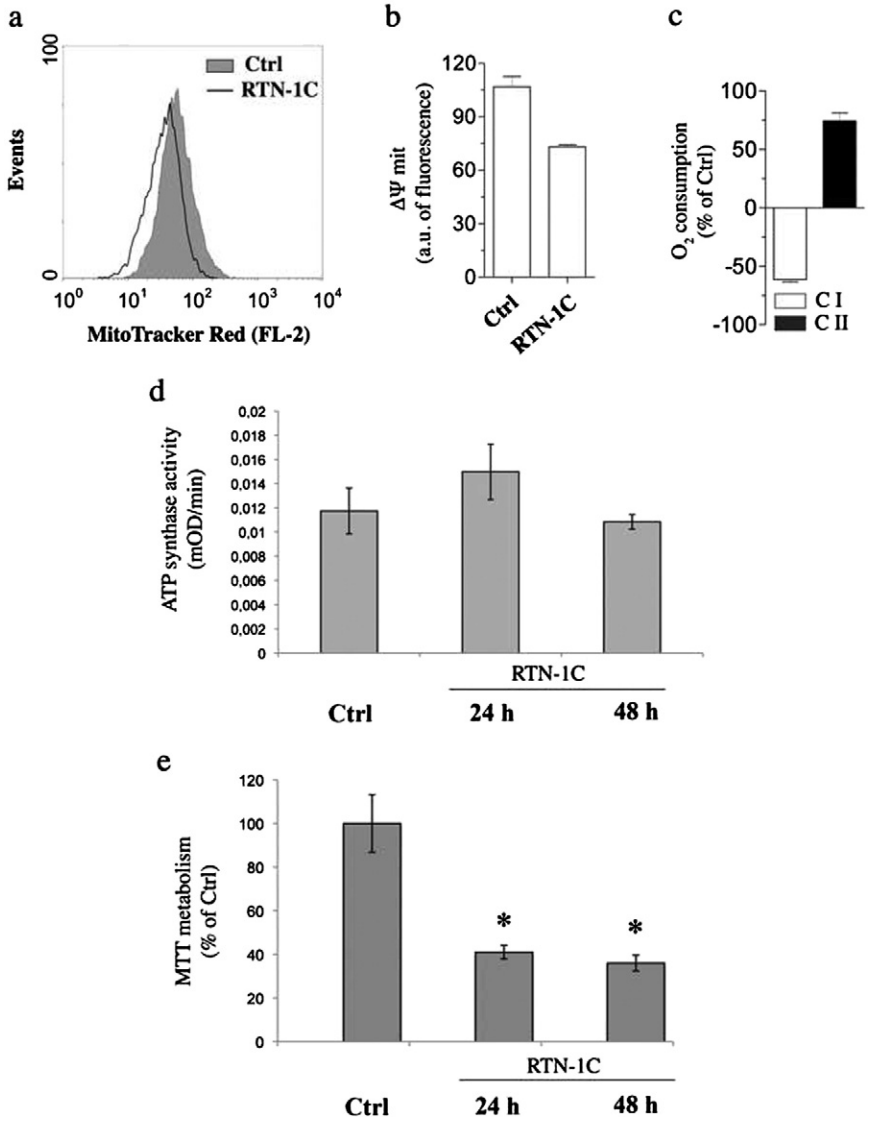

Fig. 2. RTN-1C overexpression is associated to mitochondrial defects. (a,b) SH-SY5Y wild-type (Ctrl) and SH-SY5Y^{RTN-1C} cells (48 h doxycycline induction) were incubated for 30 min with 50 nM MitoTracker Red and cytofluorometrically analyzed for Dy_m. Histograms shown are representative of three independent experiments, whose mean values ± S.D. are reported in Fig. 2b as arbitrary units (a.u.) of fluorescence. (c) Complex I and Complex II-driven oxygen consumption of RTN-1C overexpressing cells was measured by oxygraph and expressed as percentage of WT. All data are statistically significant (p values <0.01). (d) Mitochondrial ATP synthase activity measured in SH-SY5Y wild-type (Ctrl) and SH-SY5Y^{RTN-1C} cells after 24 and 48 h doxycycline induction (e) MTT assay in SH-SY5Y wild type (Ctrl) and SH-SY5Y^{RTN-1C} induced with doxycycline for the indicated times (24–48 h) to overexpress RTN-1C protein. Results are means ± SD of three independent determinations. (*) Statistically significant ($p < 0.01$) compared to control cells.

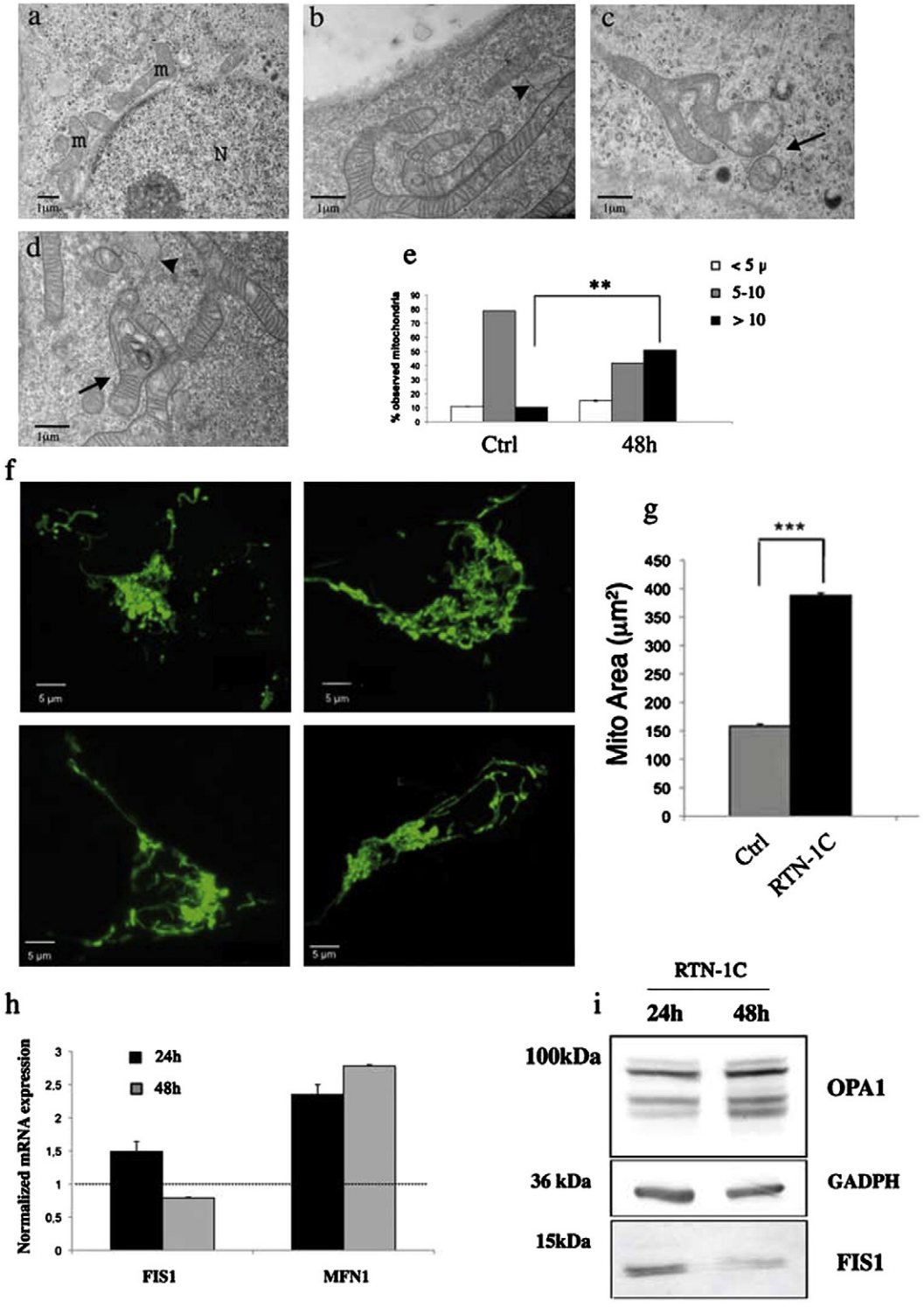

Fig. 3. RTN-1C overexpression induces ultrastructural mitochondrial alterations. (a–d) Electron microscopy analysis of SH-SY5Y wild type (a) and SH-SY5Y^{RTN-1C} cells induced with doxycycline for 48 h (b–d). Control cells showed normal shape mitochondria while RTN-1C overexpressing cells revealed the presence of elongated and swollen mitochondria with dilated and damaged cristae (arrows). ER enlargement is clearly visible in Fig. 3b and in Fig. 3d (arrowheads). (e) Quantification of mitochondria respect to their shape: normal shape (5–10 μm), elongated (>10 μm) and fragmented (<5 μm). N, nucleus, m, mitochondria. Scale bar: 1 μm**Statistically significant ($p < 0.01$) compared to control cells. (f) SH-SY5Y wild-type (upper panels) and SH-SY5Y^{RTN-1C} (lower panels) cells transfected with mito-GFP were treated with doxycycline for 48 h. Images of control mitochondria appear as individual or groups of mitochondrial tubules. At 48 h of doxycycline administration, mitochondria show fused and elongated mitochondrial tubules with a more globular structure in the soma of the cells, and long mitochondria in the neurites. Scale bar: 5 μm. (g) Quantification of mitochondrial area (GFP-signal) using Volocity software. Data were obtained from 30 cells for each experimental condition. (***) Statistically significant ($P < 0.001$) compared to control cells. (h) Real-time quantitative PCR data for SH-SY5Y^{RTN-1C} cells in response to 2 different times of induction (24 h, 48 h). The relative mRNA levels of *FIS1*, *MFN1* are expressed relative to HPRT mRNA level, used as an internal control. Results are means ± SEM of at least 3 independent determinations normalized to their relative controls. (i) SH-SY5Y-$^{RTN1-C}$ were treated with doxycycline for the indicated times (24, 48). Cell lysates were analyzed by western blot analysis for OPA1 and FIS1 expression. GADPH was used as loading controls. For Western blot analysis the results shown are representative of three independent experiments.

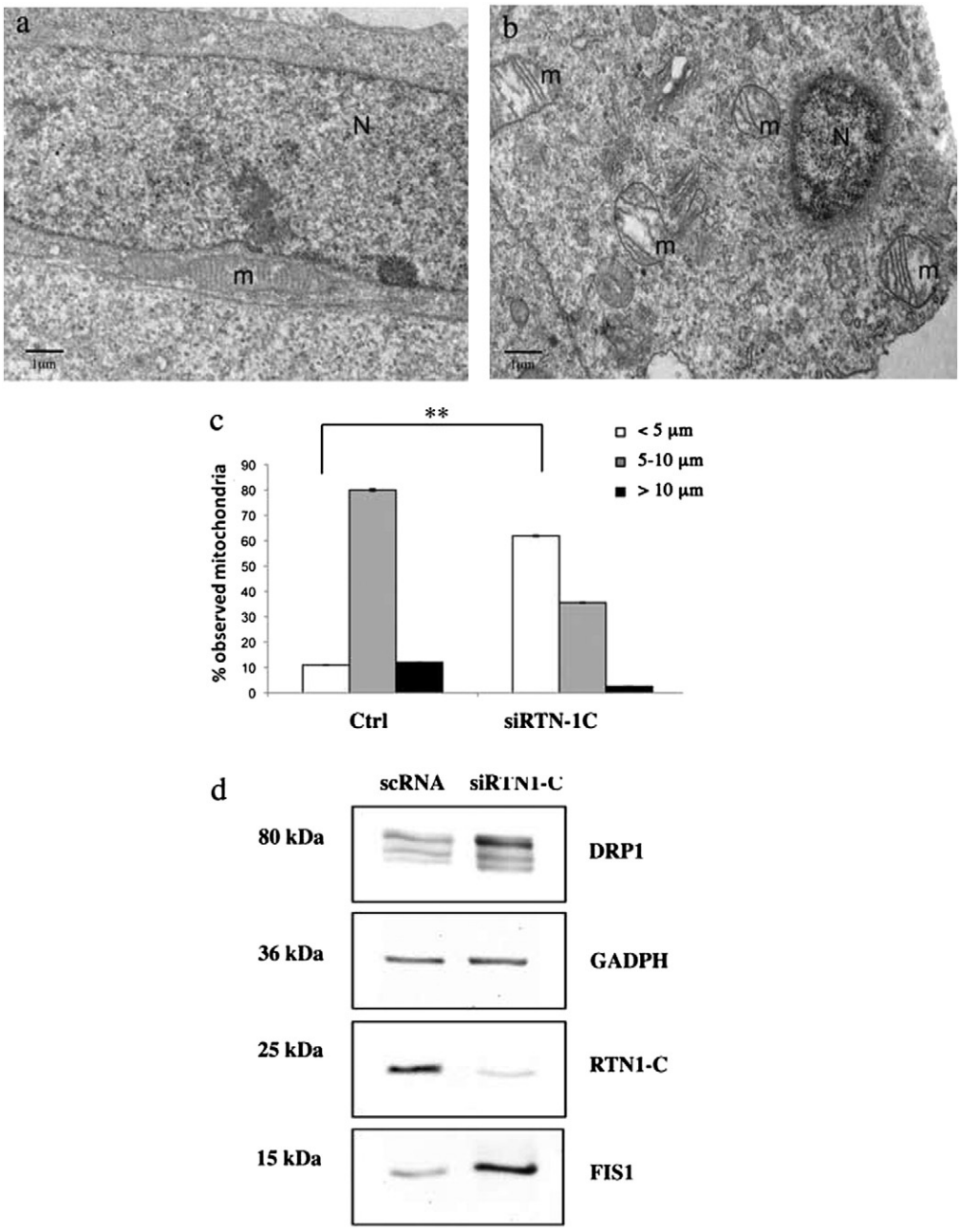

Fig. 4. SiRNA of RTN-1C results in mitochondria fragmentation. (a,b) SH-SY5Y cells were transfected with RTN-1C siRNA (b) or control (a) and analyzed by electron microscopy. RTN-1C knock down (b) resulted in numerous fragmented mitochondria (m) respect to control cells. The cristae resulted enlarged and damaged. (c) Quantification of mitochondria respect to their shape: normal shape (5–10 μm), elongated (>10 μm) and fragmented (<5 μm). N, nucleus, m, mitochondria. Scale bar: 1 μm **Statistically significant ($p < 0.01$) compared to control cells. (d) SH-SY5Y cells were transfected with RTN-1C siRNA (siRTN-1C) or control (scRNA) and cell lysates were analyzed by western blot analysis for DRP1, RTN-1C and FIS1 expression. GADPH was used as loading controls. For Western blot analysis the results shown are representative of three independent experiments.

3.3. RTN-1C modulation affects mitochondrial morphology

We set out to find whether mitochondrial functional changes observed in RTN-1C overexpressing cells depended on or were associated to any alteration of their morphology.

We analyzed the ultrastructure of neuroblastoma WT (Fig. 3a) and RTN-1C overexpressing cells (Fig. 3b–d). As expected the modulation of RTN-1C expression determined alterations of mitochondrial morphology. In particular, the organelles appeared elongated and the cristae proved to be enlarged and damaged (arrows). Mitochondria were quantified according to their size and subdivided in three categories: normal shaped (5–10 μm), elongated (>10 μm) and fragmented (<5 μm). The graph in Fig. 3E shows that about the 80% of mitochondria in WT cells displayed a normal shape while 50% of mitochondria were elongated in RTN-1C overexpressing cells.

Analysis of mitochondrial morphology by confocal microscopy revealed that while in control cells mitochondria always appeared as individual tubules or groups of interconnected ones, in the RTN-1C overexpressing cells they appeared as elongated tubules (Fig. 3f). Quantification of mitochondrial GFP signal suggested a significant increase in mitochondrial area of SH-SY5Y$^{RTN1\text{-}C}$ cells compared to control (388 ± 4.1 vs 158 ± 3.8, respectively) (Fig. 3g).

Overall these data suggest that in RTN-1C cells mitochondrial fusion machinery was deregulated. To assess this question we decided to

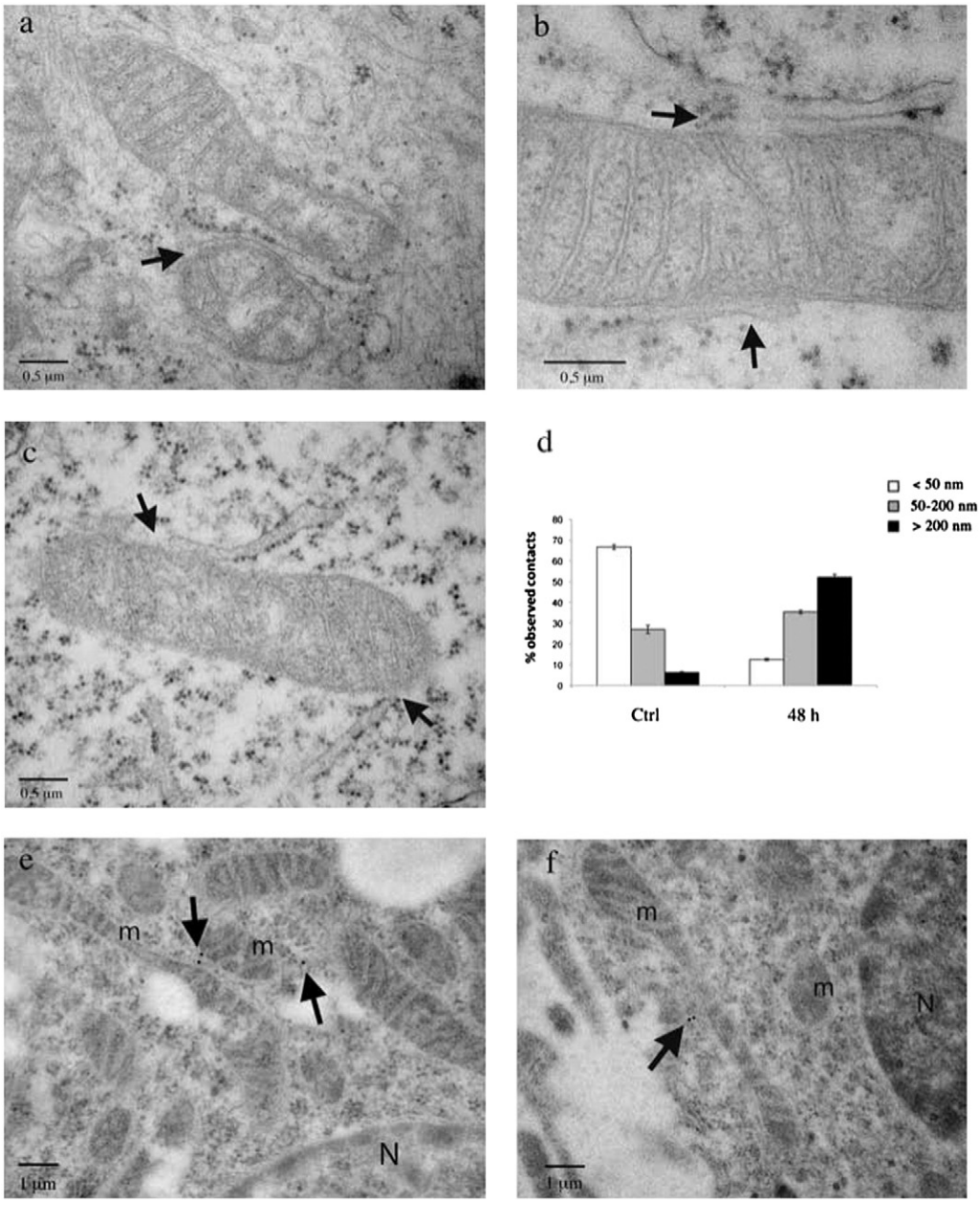

Fig. 5. Ultrastructural analysis of contact sides between ER and mitochondria. (a–c) SH-SY5Y^{RTN-1C} cells induced with doxycycline for 48 h (a,b) and SH-SY5Y wild type cells (c) were analyzed by electron microscopy in order to quantify the length of contacts between ER and mitochondria. Respect to controls the RTN-1C overexpressing cells showed an increase of contacts length (arrows). The contact sides were avoided from ribosomes. (d) Quantification of percentage of observed contacts subdivided in 'punctated' (<50 nm), 'long' (50–200 nm) and 'very long' (>200 nm). (e,f) Immunogold analysis performed to localize RTN-1C in SH-SY5Y cells. 15 nm gold particles (arrows) were visible in the contact sides between ER and mitochondria. N, nucleus, m, mitochondria. Scale bar: a, b, c 0.5 µm, e, f 1 µm.

analyze the expression of genes directly linked to the process of mitochondrial fusion.

SH-SY5Y^{RTN1C} cells were induced with doxycycline and analyzed at 24 and 48 h. In these cells, we quantified the expression levels of *FIS1* and *MFN1* using HPRT1 as internal control. The results of this analysis are shown in Fig. 3h. *FIS1* has slightly increased at 24 h but its levels were decreased at 48 h, which is consistent with the mitochondrial elongation observed at 48 h (Fig. 3f). Interestingly, *MFN1*, which is directly linked to the process of mitochondrial fusion and elongation [24], was significantly increased at the same RTN-1C induction time (Fig. 3h).

To further characterize the role of mitochondrial fusion genes we decided to also analyze FIS1 and OPA1 protein levels thus revealing the expected FIS1 decrease which is paralleled by the accumulation of OPA1 in RTN-1C overexpressing cells (Fig. 3i). Taken together these data indicate an involvement of the reticulon protein in the observed mitochondrial elongation process.

3.4. RTN-1C silencing causes mitochondrial fission

To better characterize RTN1-C's role in the maintenance of mitochondrial morphology we decided to lower its expression by mRNA silencing approach. Interestingly we obtained opposite results than in reticulon overexpressing cells. In particular the ultrastructural morphology showed that after RTN-1C down regulation mitochondria were damaged and fragmented (Fig. 4b) compared to control cells (Fig. 4a). In this condition the quantification of mitochondria on the basis of their shape (see Fig. 3e), revealed that more than 60% of organelles were fragmented (Fig. 4c); this event is paralleled by increased

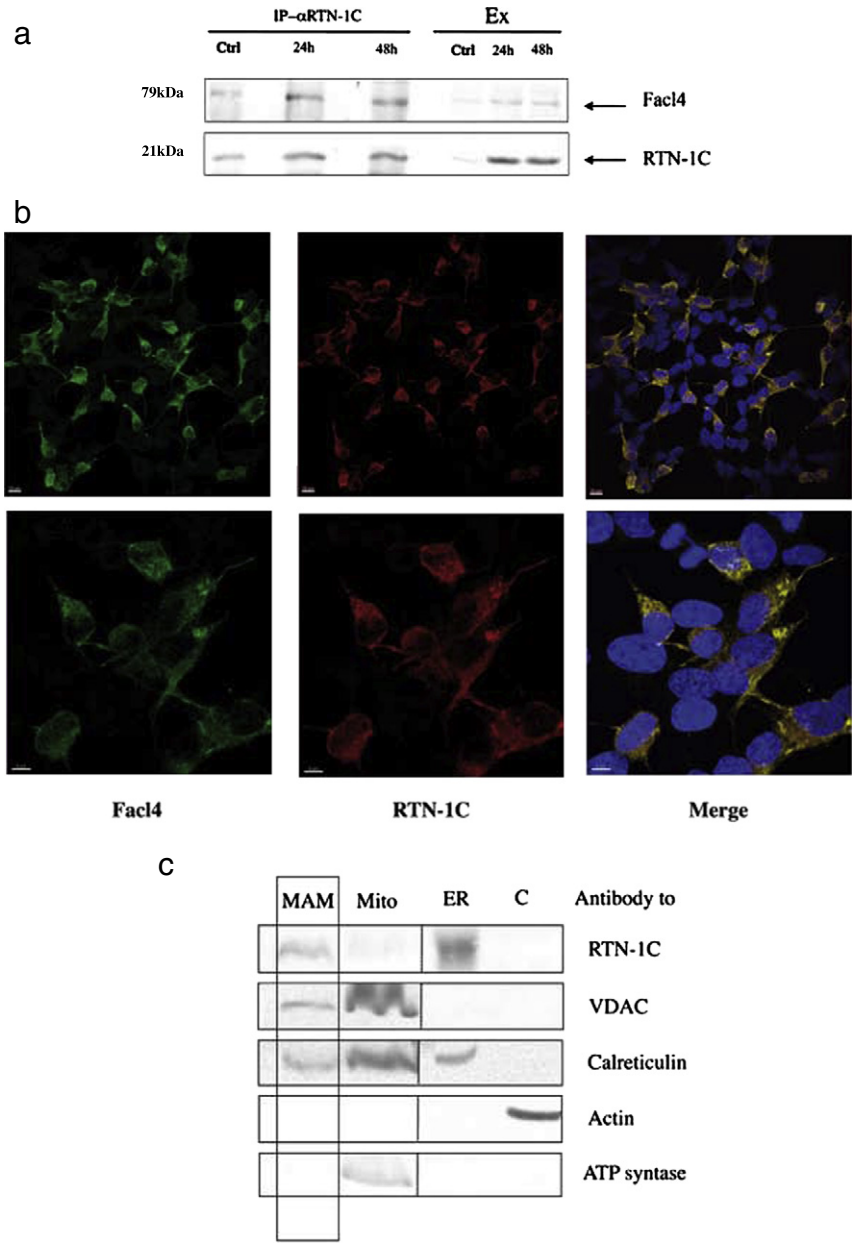

Fig. 6. RTN-1C is a component of MAM compartment. (a) Cell lysates from SH-SY5Y^{RTN-1C} cells induced with doxycycline for the indicated times were immunoprecipitated with anti-RTN-1C antibodies, and were subjected to SDS-PAGE and immunoblotting with an anti Facl4 antibody. (b) Facl4 (green) and RTN-1C (red) staining of SH-SY5Y^{RTN-1C} cells (48 h doxycycline induction) analyzed by confocal microscopy. The yellow staining in the overlaid images indicates the co-localization. Scale bars upper panels 10 μm lower panels 5 μm. (c) Protein components of subcellular fractions prepared from mouse brain homogenate. 30 μg of proteins was analyzed by immunoblot with the indicated antibodies. MAM = mitochondria-associated membrane; Mito = mitochondrial fraction; ER = endoplasmic reticulum fraction; C = cytosol.

expression of specific fission related genes i.e. DRP1 and FIS1 indicating the activation of fission processes (Fig. 4d).

3.5. RTN-1C regulates ER mitochondrial contacts

Since we showed that modulation of RTN-1C expression affected mitochondria morphology and activities we then hypothesized that the reticulon protein may localize in the MAM compartment so regulating the cross-talk between ER and mitochondria. To this end we studied ER–mitochondrial contacts in RTN1-C overexpressing cells. Indeed RTN-1C cells showed an increase in the length of mitochondrial–ER contacts as compared to control cells (Fig. 5a, c). We analyzed and quantified the contacts in the following categories: 'punctated' (<50 nm), 'long' (50–200 nm) and 'very long' (>200 nm). The quantification showed that the doxycycline treatment for 48 h induced the formation of more extended contacts between ER and mitochondria. In particular, there were more numerous 'very long' >200 nm contacts than in WT (about 10 fold), indicating an increase of physical association between the two organelles (Fig. 5d). It is interesting to note that the contact sides were free from ribosomes (Fig. 5a–c, arrows) probably to allow the physical association between mitochondria and ER.

In order to verify the presence of RTN-1C in the contact sides between ER and mitochondria, we performed immunogold staining for RTN-1C. The results showed that the gold particles were localized where ER is in contact with mitochondria (Fig. 5e,f, arrows) supporting the previous immunofluorescence observation (Fig. 1d).

3.6. RTN-1C is a component of MAM compartment

To confirm the possibility that RTN-1C is a component of the MAM compartment we decided to perform co-immunoprecipitation assay with the well known MAM-associated protein Facl4. Immunoprecipitation of RTN-1C in neuroblastoma cells revealed the association between the two proteins (Fig. 6a); this is further confirmed by immunofluorescence analysis of RTN-1C and Facl4 (Fig. 6b). Similar results were obtained with VDAC MAM associated protein (data not shown). Finally, in order to clearly demonstrate

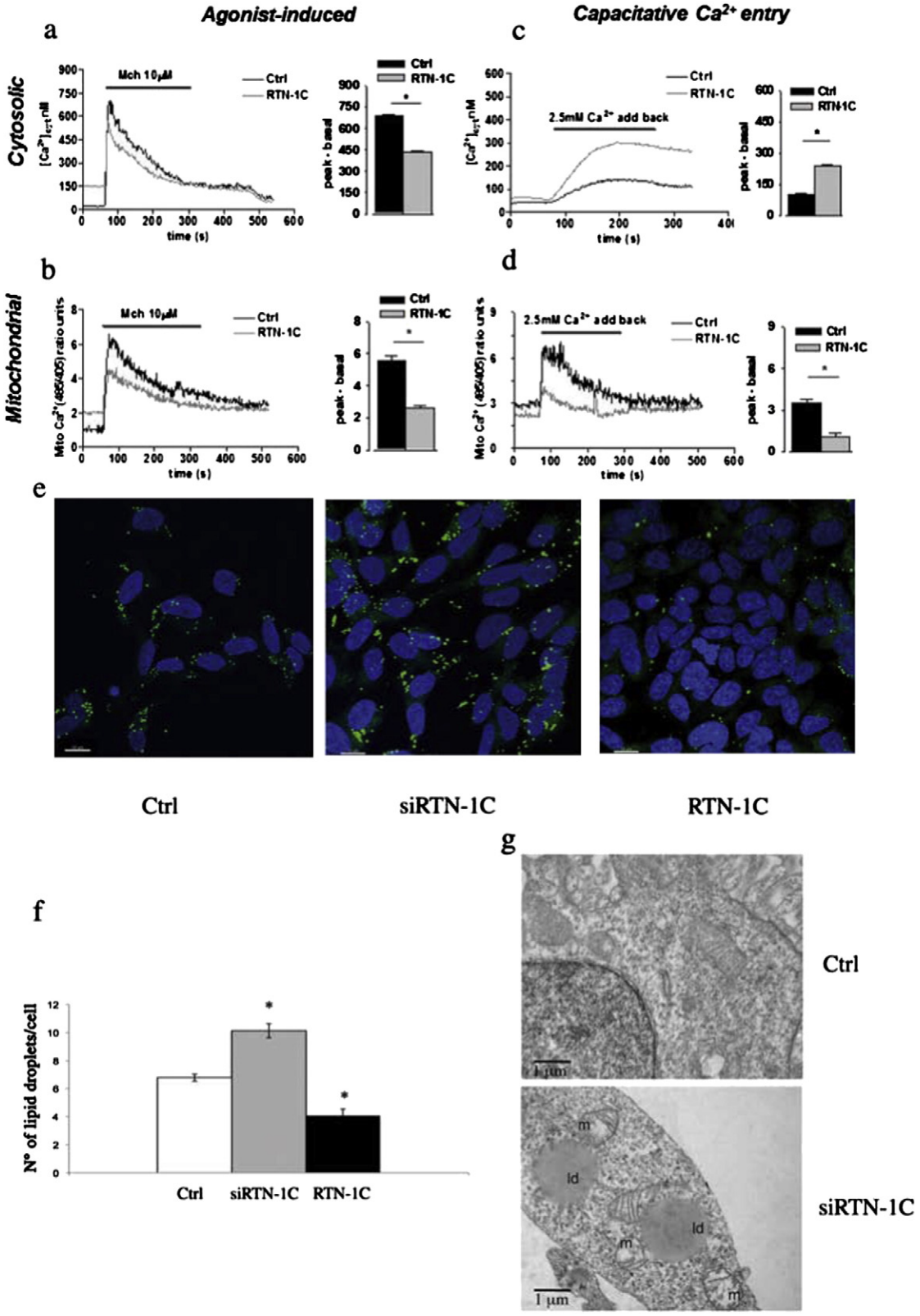

the association of RTN-1C with the MAM compartment we performed subcellular fractionation to isolate ER, MAM and mitochondria. The results obtained by immunoblot analysis of the different fractions by specific antibodies showed the presence of the reticulon protein in the MAM compartment as well as in the endoplasmic reticulum one (Fig. 6c). Taken together these data clearly indicated RTN-1C protein as a molecular component of the MAM compartment.

3.7. RTN-1C affects mitochondrial Ca^{2+} responses and lipid exchange with the ER compartment

Recent studies indicated that MAM are very important for a correct communication between ER and mitochondria. In particular it has been demonstrated that MAM are crucial for intracellular calcium homeostasis and for synthesis and transport of phospholipids.

We have previously shown that overexpression of RTN-1C resulted in elevated cytosolic Ca^{2+} levels [17]. Prompted by this finding, we set out to characterize calcium homeostasis both at the cytosolic and mitochondrial level. Ca^{2+} imaging experiments were performed on SH-SY5Y cells overexpressing RTN-1C. The mean (peak–basal) cytosolic Ca^{2+} concentrations generated by control and RTN-1C overexpressing cells after stimulation with the muscarinic receptor agonist methacholine (Mch, 10 μM) were 684 ± 11 nM and 430 ± 14 nM, respectively (Fig. 7a). However, basal Ca^{2+} levels were significantly higher in RTN-1C overexpressing cells compared to controls (150 ± 14 and 30 ± 16 nM, respectively) (Fig. 7a). To assess the effect of RTN-1C overexpression on mitochondrial Ca^{2+} signals, a similar protocol was applied on 2mtRP and RTN-1C co-transfected cells (Fig. 7b). Despite increased basal Ca^{2+} levels, RTN-1C overexpressing cells generated lower mitochondrial Ca^{2+} signals whose mean (peak–basal) values were 2.6 ± 0.2 ratio units compared to 5.6 ± 0.1 ratio units of control cells (Fig. 7b). To understand how RTN-1C overexpression would modulate the capacitative calcium entry and the subsequent mitochondrial Ca^{2+} uptake, cells were treated with a capacitative Ca^{2+} entry protocol. The mean (peak–basal) values for cytosolic Ca^{2+} signal generated by Ca^{2+} add back in RTN-1C overexpressing cells compared to control were 234 ± 15 and 98 ± 12 nM, respectively (Fig. 7c). We used the same protocol to assess the effect of RTN-1C overexpression on mitochondrial Ca^{2+} signals. Mean (peak–basal) values in RTN-1C overexpressing cells compared to control were 1.1 ± 0.2 and 3.5 ± 0.3 ratio units, respectively (Fig. 7d). Overall these data suggest that RTN-1C perturbs intracellular Ca^{2+} homeostasis and in particular alters mitochondrial calcium up-take. Accordingly, to assess whether RTN-1C affects the expression levels of ER pumps and channels we measured the relative mRNA levels of RyR2, SERCA2b, IP3RT1, and MFN2. Data obtained indicated that neither SERCA pumps, nor IP3RT1 or MFN2 changed but we found increased expression levels of RyR2 (Supplementary Fig. 1).

Phospholipid exchange between ER and mitochondria is another cellular process in which the MAM compartment play an important role [25], such exchange also beeing involved in mitochondrial membrane morphogenesis. Considering the effect of RTN-1C protein on mitochondrial morphological changes previously described we wondered whether this event was coupled to any perturbation of lipid trasport between ER and mitochondria.

Lipid quantification was performed by BODIPY staining and fluorescence analysis. Fig. 7e showed that RTN-1C modulation results in a significative change in lipid content; in particular RTN-1C overexpression is accompanied by a decrease in lipid content while RTN-1C down regulation induces an evident lipid droplets accumulation (Fig. 7f). SiRTN-1C cells were further analyzed by electon microscopy showing a dramatic accumulation of lipids droplets (Fig. 7g).

4. Discussion

MAM is a dynamic ER subcompartment connecting endoplasmic reticulum to mitochondria. It is well known that any alteration of ER–mitochondria connection may result in dysregulation of mitochondrial function [26,27], in the context of physiological and pathological events. We have previously demonstrated that RTN-1C overexpressing cells exhibited ultrastructural changes affecting endoplasmic reticulum as well as mitochondria [17].

Prompted by this evidence and considering the fact that, in this study, among the various RTN-1C interactors we identified mitochondrial ATP synthase, we decided to investigate the role of RTN-1C protein in mitochondrial dynamics. We demonstrated that reticulon overexpression affected mitochondrial transmembrane potential and oxygen consumption at the level of Complex I and Complex II. Interestingly the ATP production was likely maintained by the adjustment of oxidative phosphorylation. These data suggest that an RTN-1C dependent perturbation in the ER compartment has a significant impact on the mitochondrial one. Consistently, analysis of mitochondrial dynamics by confocal and electron microscopy revealed abnormalities of mitochondrial morphology. In fact, RTN-1C overexpression triggered mitochondrial elongation, paralleled by derangement of the mitochondrial fusion machinery. Our results are in line with recent data demonstrating that during different stress conditions mitochondria elongate to sustain cellular ATP levels and promote viability [28,29]. Interestingly, when we performed RTN-1C siRNA experiments we observed opposite events i.e. mitochondrial fragmentation and activation of fission processes, thus confirming the close correlation between ER shaping reticulon protein expression and mitochondria shape.

It has been demonstrated that the maintaining of mitochondrial structure also depends on their functional contacts with endoplasmic reticulum [30]. Sutendra et al. reported that overexpression of another reticulons family member (Nogo-B) increased the distance between the ER and mitochondria [31]. Therefore, it could be speculated that RTN-1C overexpression could contribute to structuring ER–mitochondria contact sites. Actually when we analyzed and quantified the different categories of contacts (punctate, long, very long) between ER and mitochondria we detected an increase of physical association between the two organelles in RTN-1C overexpressing cells. Moreover, we highlighted the specific localization of reticulon-1C protein at the level

Fig. 7. RTN-1C modulation alters calcium and lipids exchange between ER and mitochondria.Agonist-induced cytosolic (a) and mitochondrial (b) Ca^{2+} signals in RTN-1C overexpressing SH-SY5Y cells. For cytosolic measurements, control and RTN-1C overexpressing cells were loaded with fura-2 (2 μM, 1 h) and perfused with Mch (10 μM). Data are representative of at least 100 cells, from 3 experiments for each condition. For mitochondrial measurements, 2mtRP and RTN-1C co-transfected cells together with controls were treated with the same protocol as above. Data are representative of at least 50 cells, from 8 experiments for each condition. Bars show quantification of Ca^{2+} responses (peak–basal) in response to Mch application. Cytosolic (c) and mitochondrial (d) Ca^{2+} signals following capacitative Ca^{2+} entry protocol in RTN-1C overexpressing SH-SY5Y cells. For cytosolic measurements, cells were loaded with fura-2 (2 μM, 1 h) and were pretreated with thapsigargin (5 μM) for 15–30 min. Next, cells were perfused with Ca^{2+} free-KHB for the first 30 s, then Ca^{2+} was added back at a concentration of 2.5 mM for 5 min. Data are representative of at least 80 cells from 3 experiments for each condition. For mitochondrial measurements, cells were co-transfected with 2mtRP and RTN-1C and recordings were carried out using the same protocol as above. Data are representative of 45 to 50 cells from 4 to 5 experiments. Bars show quantification of Ca^{2+} responses (peak-basal) to Ca^{2+} addition. (*) Statistically significant ($P < 0.05$; unpaired Student's t test). (e) SH-SY5Y wild type, RTN-1C siRNA and SH-SY5Y$^{RTN\text{-}1C}$ cells (48 h doxycycline induction) were stained with BODIPY and Hoechst and analyzed by confocal microscopy. RTN-1C down regulation results in an evident accumulation of lipid droplets while its overexpression is paralleled by a significant decrease in lipid content. Scale bars 10 μm. (f) Quantification of lipid content expressed as number of spots per cell. (g) Electron microscopy analysis of SH-SY5Y cells after RTN-1C knock down showing numerous lipid droplets respect to control cells (Ctrl) m, mitochondria, ld, lipid droplet. Scale bar: 1 μm.

of ER–mitochondria contact points. On the basis of this evidence, we predicted that RTN1-C was a key component of MAM compartment. Importantly, we revealed that RTN-1C participates in the molecular components of MAM as demonstrated by the co-localization and the physical association with well known ER and mitochondria associated protein (i.e. VDAC and Facl4, [32]. This finding also explains the observed role of RTN-1C protein in the regulation of mitochondrial biogenesis. Although a growing body of evidence indicates that ER–mitochondria interaction could strongly influence fission and fusion [33,34], in order to maintain the correct mitochondrial morphology and function, little is known about the molecular components involved in this process. The results reported in our work indicated that RTN-1C is a key component of the MAM compartment; as such, it is able to play an important role in the mitochondrial dynamics. This finding might further deepen our understanding of the pathogenesis of various diseases known to involve MAM dysfunction such as neurodegenerative diseases [35,36].

The main cellular functions of MAM are calcium signaling and lipid trafficking between ER and mitochondria [30]. Thus considering the data here obtained we expected that these two processes are deregulated by RTN-1C modulation.

We actually found that RTN-1C overexpressing cells exhibited enhanced capacitative Ca^{2+} entry but reduced mitochondrial Ca^{2+} uptake. As the contact between ER and mitochondria is essential for the coordination of Ca^{2+} transfer [37], it could be speculated that the observed impaired ER–mitochondria contact sites, related to RTN-1C protein, could affect mitochondrial efficiency in Ca^{2+} uptake [38]. On the basis of previous data, we hypothesized that mitochondrial Ca^{2+} mishandling may be associated with changes at mitochondrial structural and functional levels. We have also analyzed the expression levels of different calcium pumps and channels highlighting the up regulation of RyR2. Although further experiments are required to dissect the association between RTN-1C overexpression and RYR2 up-regulation it is interesting to note that a recent report indicated the important role of RyR in mitochondrial Ca^{2+} uptake mechanism in neurons [39]. We can hypothesize that this up-regualtion may be due to the already documented increase in cytosolic Ca^{2+} levels induced by RTN-1C protein [17].

Recently Voss et al. reported that in *S. cerevisiae* ER-shaping proteins play a role in maintaining functional contacts between ER and mitochondria. Moreover, they suggested that the shape of the ER at the level of MAM regulates lipid exchange between these two organelles [40]. According to this observation, we demonstrated that modulation of RTN-1C expression resulted in a significant change in lipid content. Particularly relevant is the accumulation of lipid droplets observed in RTN-1C knock down cells, thus supporting the notion that the reticulon protein is essential for proper lipid trafficking.

5. Conclusion

In conclusion, considering the emergence of the important role of the cross-talk between ER and mitochondria both in physiological and pathological events the present work indicates that RTN-1C is a key component of MAM compartment. As such, it might regulate mitochondrial function and dysfunction, thus providing a possible mechanism by which this structural ER protein modulates the cellular stress.

Supplementary data to this article can be found online at http://dx.doi.org/10.1016/j.bbamcr.2014.12.031.

Conflict of interest

I wish to confirm that there are no known conflicts of interest associated with this publication and there has been no significant financial support for this work that could have influenced its outcome.

Acknowledgments

Thanks are due to Elena Romano and Emanuela Viaggiu for technical advice and to Nicoletta Paolillo for advices with RT-PCR.

This work was supported by AIRC grants to FD (MFAG 11440) and GMF (IG2102). This study has been partially supported by grants from MIUR (PRIN 2012 and FIRB) and from the Ministry of Health of Italy 'Ricerca Corrente' and 'Ricerca Finalizzata' and AIRC (IG11409) to MP. The support of the EU grant 'Transpath' Marie Curie project (289964) to MP is also acknowledged. None of the authors has actual or potential conflicts of interest.

References

[1] D.E. Copeland, A.J. Dalton, An association between mitochondria and the endoplasmic reticulum in cells of the pseudobranch gland of a teleost, J. Biophys. Biochem. Cytol. 5 (1959) 393–396.
[2] D.J. Morré, W.D. Merritt, C.A. Lembi, Connections between mitochondria and endoplasmic reticulum in rat liver and onion stem, Protoplasma 73 (1971) 43–49.
[3] J.E. Vance, Phospholipid synthesis in a membrane fraction associated with mitochondria, J. Biol. Chem. 265 (1990) 7248–7256.
[4] O. Camici, L. Corazzi, Import of phosphatidylethanolamine for the assembly of rat brain mitochondrial membranes, J. Membr. Biol. 148 (1995) 169–176.
[5] T. Hayashi, R. Rizzuto, G. Hajnoczky, T.P. Su, MAM: more than just a housekeeper, Trends Cell Biol. 19 (2009) 81–88.
[6] J.E. Vance, Molecular and cell biology of phosphatidylserine and phosphatidylethanolamine metabolism, Prog. Nucleic Acid Res. Mol. Biol. 75 (2003) 69–111.
[7] G. Csordás, P. Várnai, T. Golenár, et al., Imaging interorganelle contacts and local calcium dynamics at the ER–mitochondrial interface, Mol. Cell 39 (2010) 121–132.
[8] Y.B. Ouyang, R.G. Giffard, ER–mitochondria crosstalk during cerebral ischemia: molecular chaperones and ER–mitochondrial calcium transfer, Int. J. Cell Biol. 493934 (2012). http://dx.doi.org/10.1155/2012/493934.
[9] E.A. Schon, E. Area-Gomez, Mitochondria-associated ER membranes in Alzheimer disease, Mol. Cell. Neurosci. 55 (2013) 26–36.
[10] G. Hajnóczky, E. Davies, M. Madesh, Calcium signaling and apoptosis, Biochem. Biophys. Res. Commun. 304 (2003) 445–454.
[11] D. Ron, P. Walter, Signal integration in the endoplasmic reticulum unfolded protein response, Nat. Rev. Mol. Cell Biol. 8 (2007) 519–529.
[12] S.A. Detmer, D.C. Chan, Functions and dysfunctions of mitochondrial dynamics, Nat. Rev. Mol. Cell Biol. 8 (2007) 870–879.
[13] G. Twig, B. Hyde, O.S. Shirihai, Mitochondrial fusion, fission and autophagy as a quality control axis: the bioenergetic view, Biochim. Biophys. Acta 1777 (2008) 1092–1097.
[14] L.C. Gomes, L. Scorrano, Mitochondrial elongation during autophagy: a stereotypical response to survive in difficult times, Autophagy 7 (2011) 1251–1253.
[15] F.Y. Teng, B.L. Tang, Cell autonomous function of Nogo and reticulons: the emerging story at the endoplasmic reticulum, J. Cell. Physiol. 216 (2008) 303–308.
[16] F. Di Sano, B. Fazi, G. Citro, P.E. Lovat, G. Cesareni, M. Piacentini, Glucosylceramide synthase and its functional interaction with RTN-1C regulate chemotherapeutic-induced apoptosis in neuroepithelioma cells, Cancer Res. 63 (2003) 3860–3865.
[17] F. Di Sano, B. Fazi, R. Tufi, R. Nardacci, M. Piacentini, Reticulon-1C acts as a molecular switch between endoplasmic reticulum stress and genotoxic cell death pathway in human neuroblastoma cells, J. Neurochem. 102 (2007) 345–353.
[18] A.B. Perdomo, F. Ciccosanti, O.L. Iacono, et al., Liver protein profiling in chronic hepatitis C: identification of potential predictive markers for interferon therapy outcome, J. Proteome Res. 11 (2012) 717–727.
[19] C. Montaldo, S. Mattei, A. Baiocchini, et al., Spike-in SILAC proteomic approach reveals the vitronectin as an early molecular signature of liver fibrosis in hepatitis C infections with hepatic iron overload, Proteomics 14 (2014) 1107–1115.
[20] S. Di Bartolomeo, M. Corazzari, F. Nazio, et al., The dynamic interaction of AMBRA1 with the dynein motor complex regulates mammalian autophagy, J. Cell Biol. 191 (2010) 155–168.
[21] M.R. Wieckowski, C. Giorgi, M. Lebiedzinska, J. Duszynski, P. Pinton, Isolation of mitochondria-associated membranes and mitochondria from animal tissues and cells, Nat. Protoc. 4 (2009) 1582–1590.
[22] G. Filomeni, G. Cerchiaro, A.M. Da Costa Ferreira, et al., Pro-apoptotic activity of novel Isatin-Schiff base copper(II) complexes depends on oxidative stress induction and organelle-selective damage, J. Biol. Chem. 282 (2007) 12010–12021.
[23] M. Corazzari, P.E. Lovat, J.L. Armstrong, et al., Targeting homeostatic mechanisms of endoplasmic reticulum stress to increase susceptibility of cancer cells to fenretinide-induced apoptosis: the role of stress proteins ERdj5 and ERp57, Br. J. Cancer 96 (2007) 1062–1071.
[24] K.L. Cerveny, Y. Tamura, Z. Zhang, R.E. Jensen, H. Sesaki, Regulation of mitochondrial fusion and division, Trends Cell Biol. 17 (2007) 563–569.
[25] W.A. Prinz, Lipid trafficking sans vesicles: where, why, how? Cell 143 (2010) 870–874.
[26] B. Kornmann, C. Osman, P. Walter, The conserved GTPase Gem1 regulates endoplasmic reticulum–mitochondria connections, Proc. Natl. Acad. Sci. U. S. A. 108 (2011) 14151–14156.
[27] K. Hirai, G. Aliev, A. Nunomura, et al., Mitochondrial abnormalities in Alzheimer's disease, J. Neurosci. 21 (2001) 3017–3023.

[28] L.C. Gomes, G. Di Benedetto, L. Scorrano, During autophagy mitochondria elongate, are spared from degradation and sustain cell viability, Nat. Cell Biol. 13 (2011) 589–598.
[29] D.B. Wang, T. Uo, C. Kinoshita, et al., Bax interacting factor-1 promotes survival and mitochondrial elongation in neurons, J. Neurosci. 34 (2014) 2674–2683.
[30] M. Lebiedzinska, G. Szabadkai, A.W. Jones, et al., Interactions between the endoplasmic reticulum, mitochondria, plasma membrane and other subcellular organelles, Int. J. Biochem. Cell Biol. 41 (2009) 1805–1816.
[31] G. Sutendra, P. Dromparis, P. Wright, et al., The role of Nogo and the mitochondria–endoplasmic reticulum unit in pulmonary hypertension, Sci. Transl. Med. 3 (2011) 88ra55. http://dx.doi.org/10.1126/scitranslmed.3002194.
[32] A.R. van Vliet, T. Verfaillie, P. Agostinis, New functions of mitochondria associated membranes in cellular signaling, Biochim. Biophys. Acta (2014). http://dx.doi.org/10.1016/j.bbamcr (pii: S0167-4889(14)00093-7).
[33] S. Marchi, S. Patergnani, P. Pinton, The endoplasmic reticulum–mitochondria connection: one touch, multiple functions, Biochim. Biophys. Acta 2014 (1837) 461–469.
[34] F. Korobova, V. Ramabhadran, H.N. Higgs, An actin-dependent step in mitochondrial fission mediated by the ER-associated formin INF2, Science 339 (2013) 464–467.
[35] E. Area-Gomez, M. Del Carmen Lara Castillo, M.D. Tambini, et al., Upregulated function of mitochondria-associated ER membranes in Alzheimer disease, EMBO J. 31 (2012) 4106–4123.
[36] E.A. Schon, E. Area-Gomez, Is Alzheimer's disease a disorder of mitochondria-associated membranes? J. Alzheimers. Dis. 20 (2010).
[37] A.A. Rowland, G.K. Voeltz, Endoplasmic reticulum-mitochondria contacts: function of the junction, Nat. Rev. Mol. Cell Biol. 13 (2012) 607–625.
[38] R. Rizzuto, T. Pozzan, Microdomains of intracellular Ca2+: molecular determinants and functional consequences, Physiol. Rev. 86 (2006) 369–408.
[39] R. Jakob, G. Beutner, V.K. Sharma, Y. Duan, R.A. Gross, S. Hurst, B.S. Jhun, J. O-Uchi, S.S. Sheu, Molecular and functional identification of a mitochondrial ryanodine receptor in neurons, Neurosci. Lett. 575 (2014) 7–12.
[40] C. Voss, S. Lahiri, B.P. Young, C.J. Loewen, W.A. Prinz, ER-shaping proteins facilitate lipid exchange between the ER and mitochondria in S. cerevisiae, J. Cell Sci. 125 (2012) 4791–4799.